Serrano, D., Golpour, I. & Sánchez-Delgado, S. (2020). Predicting the effect of bed materials in bubbling fluidized bed gasification using artificial neural networks (ANNs) modeling approach. *Fuel*, 266, 117021.

DOI: 10.1016/j.fuel.2020.117021

Predicting the effect of bed materials in bubbling fluidized bed gasification using artificial neural networks (ANNs) modeling approach

Daniel Serrano[a*], Iman Golpour[b], Sergio Sánchez-Delgado[a]

[a]*Energy System Engineering Research Group, Thermal and Fluid Engineering Department, Carlos III University of Madrid, Leganés, Madrid, Spain*

[b]*Department of Mechanical Engineering of Biosystems, Urmia University, Urmia, Iran*

*T: +34916248884; E-mail: daserran@ing.uc3m.es

Abstract

The effect of different bed materials was included a as new input into an artificial neural network model to predict the gas composition (CO_2, CO, CH_4 and H_2) and gas yield of a biomass gasification process in a bubbling fluidized bed. Feed and cascade forward back propagation networks with one and two hidden layers and with Levenberg-Marquardt and Bayesian Regulation learning algorithms were employed for training of networks. A high number of network topologies were simulated to determine the best configuration. It was observed that the developed models are able to predict the CO_2, CO, CH_4, H_2 and gas yield with good accuracy ($R^2 > 0.94$ and MSE $< 1.7\times10^{-3}$). The results obtained indicate that this approach is a powerful tool to help in the efficient design, operation and control of bubbling fluidized bed gasifiers working with different operating conditions, including the effect of the bed material.

Keywords: gasification; bubbling fluidized bed; bed material; artificial neural network

1. Introduction

Biomass gasification is a highly efficient thermochemical conversion process that converts different biomass feedstocks into a raw gas mainly composed by H_2, CO, CO_2, CH_4 and light hydrocarbons which can be used in further applications such as fuel or for producing chemicals (Puig-Arnavat et al., 2013). This thermochemical process is a good option to transform different types of residues into valuable products to produce energy. Thereby, energy is produced in a renewable way and the problem of residues disposal is reduced. Among the different techniques used to study this process, modelling is a valuable tool to design and obtain a first approximation to the expected results, reducing the experimental and human cost. Different kinds of models, including thermodynamic equilibrium, kinetic rate, computational fluid dynamic (CFD) and artificial neural network (ANN) have been improved for studying and modelling the gasification processes (Ahmed et al., 2012; Baruah and Baruah, 2014; Puig-Arnavat et al., 2010).

Equilibrium models are based on the concept of chemical reaction equilibrium based on the second law of thermodynamics, considering also the transfer phenomena between phases and the reaction kinetics of the primary reactions (Karmakar and Datta, 2011; Mahishi and Goswami, 2007). In CFD models, a set of equations for mass, momentum and energy conservation are solved simultaneously along the gasifier to predict the distribution of different parameters such as temperature or species concentration (Baruah and Baruah, 2014).

The design of new products and processes is a challenge to researchers who face to high cost and time-consuming experiments to obtain reliable information for different operating conditions. The advances in soft computing and computer science enhance the interest in the development of prediction models for time consuming and costly experiments (Ayodele and Cheng, 2015). To overcome these concerns, artificial intelligence systems such as ANNs are a reliable tool for the prediction of nonlinear system data due to its accuracy, precision and low cost and time consuming.

ANN analysis is a recent approach for the prediction of the gasification outputs in which a neural network learns by itself from different sets of experimental data simulating the human brain in terms of mathematical functions. The theory of the ANN is based in the analogy with the human brain, which is composed by numerous elements called neurons organized in different layers. These neurons are interconnected and exchange information between them. When different stimulus or inputs are received by the neurons, they modify their state and transfer the information to the next neuron. This way the information travels across the different layers of neurons until a final response for the initial inputs is obtained. In order to obtain the final response, the neural network needs to learn and recognize the relationships between inputs and outputs, in the same way humans do. Thus, an ANN is formed by an input layer, a number of hidden layers and an output layer, being the number of neurons per layer a parameter that can be modified. As a modern approach, ANNs are particularly useful to obtain the solution of an extensive variety of problems in science and engineering, being the prediction performance and generalization closely related with the training of the network. This tool have an excellent learning ability and a high capability for recognizing and modeling complex non-linear relations between the input and the output variables of a process (Mikulandrić et al., 2014). These characteristics make ANNs very interesting and useful, motivating their use in the modeling of biomass gasification processes. Therefore, biomass gasification, which is a complex thermochemical process, can be conveniently simulated using the appropriately designed ANN.

The application of ANN in biomass pyrolysis and gasification processes have also been reported by (Karaci et al., 2016; Souza et al., 2012; Sreejith et al., 2013; Sunphorka et al., 2017; Xiao et al., 2009). ANN based models were developed for predicting the product yield and gas composition in an atmospheric steam blow biomass fluidized bed gasifier (Guo et al., 2001). It was concluded that the feed forward neural network model had better predictive accuracy over traditional regression models. Chavan et al. used two types of ANN based data-driven models for the prediction of the gas heating value and production in coal gasifiers (Chavan et al., 2012). Mikulandrić et al. simulated a fixed bed gasifier using an ANN from experimental data, showing the capability of this tool to predict the results of a gasification process with acceptable accuracy and speed (Mikulandrić et al., 2014). Puig-Arnavat et al. obtained similar conclusions for the prediction of the gas composition in circulating and bubbling fluidized beds using ANN (Puig-Arnavat et al., 2013). Baruah et al. also developed a ANN-based model for the prediction of the gas composition in a down-draft fixed bed gasifier, suing C, H, O, ash and moisture contents for the biomass and reduction zone temperature as inputs (Baruah et al., 2017). Pandey et al. predicted the performance of municipal solid waste gasification in terms of lower heating value of the gas and products, and gas yield (Pandey et al., 2016a). Recently, Shahbaz et al. also used the ANN approach for the studying the steam gasification of palm oil waste using bottom ash and CaO, obtaining a good prediction compared to experimental data (Shahbaz et al., 2019).

All the mentioned studies, used similar input data for the models based on the biomass properties (C, H, O, moisture and ash content) and operating conditions (temperature, equivalence ratio and steam/biomass ratio). However, a lot of work has been done using different bed materials in the fluidized bed in order to improve the product gas quality (Arena and Di Gregorio, 2014; Baratieri et al., 2010; Gómez-Barea et al., 2005). Although ANN based modeling have been used in biomass gasification, to the authors' knowledge, no study has focused in the prediction, using ANN and different bed materials, of a bubbling fluidized bed gasifier. This is parameter has an important influence in the products from the gasifier and is usually skipped from this type of approaches. Hence, the objective of the present work is to develop ANN models for the prediction of the producer gas composition and gas yield for several operating conditions in bubbling fluidized bed gasifiers using different bed materials. The addition of this new input data to the previous models is studied in order to get a more complete model for future predictions or, if, on the contrary, it results in a very complicated model that cannot obtain a relation between the input and output data.

2. Material and methods

2.1. Artificial neural network (ANN) design

In this study, the Neural Network Toolbox from MATLAB software R2018b was used to design and train the ANN, validating the obtained results. Figure 1 shows the topology of developed neural network with the input and output variables. Nine input parameters were selected for this work: carbon (C), hydrogen (H), oxygen (O), moisture (MC) and ash (Ash) contents for the biomass, equivalence ratio (ER), reaction temperature (T), steam/biomass mass ratio (S/B), and bed material. The first eight inputs are the usually employed in this type of studies as the give important information about the type of biomass and the most important operating conditions. The ninth input variable is added in this work as it also has an important relation with the final composition of the product gas and it is usually avoided in gasification ANN models. This variable has been accounted as a discrete variable ranging from 1 to 4, corresponding each value to one different bed material. This way, the network can be able to distinguish between bed materials. In the case of the outputs, five variables have been considered separately (i.e.: one ANN per output): H_2, CO, CO_2, CH_4 and gas yield (GY). The experimental data needed for the ANN have been collected from previous biomass gasification experiments of the authors (Serrano et al., 2017, 2016) and completed with more experimental data collected from literature, using all of them a fluidized bed gasifier (Arena et al., 2010; Arena and Di Gregorio, 2014; Baratieri et al., 2010; Campoy Naranjo, 2009; Christodoulou et al., 2014; De Andrés et al., 2011a, 2011b; Gómez-Barea et al., 2005; Huynh and Kong, 2013; Kaewluan and Pipatmanomai, 2011b, 2011a; Lahijani and Zainal, 2011; Lan et al., 2019; Loha et al., 2013; Lv et al., 2004; Mansaray et al., 1999; Miccio et al., 2009; Narváez et al., 1996; Pandey et al., 2016b; Roche et al., 2014). Table 1 shows the boundaries and levels for the nine inputs and five outputs used in this study. The range of this variables in addition to the type of gasifier (fluidized bed) and gasifying agent (air), defines the range of validity of the present model.

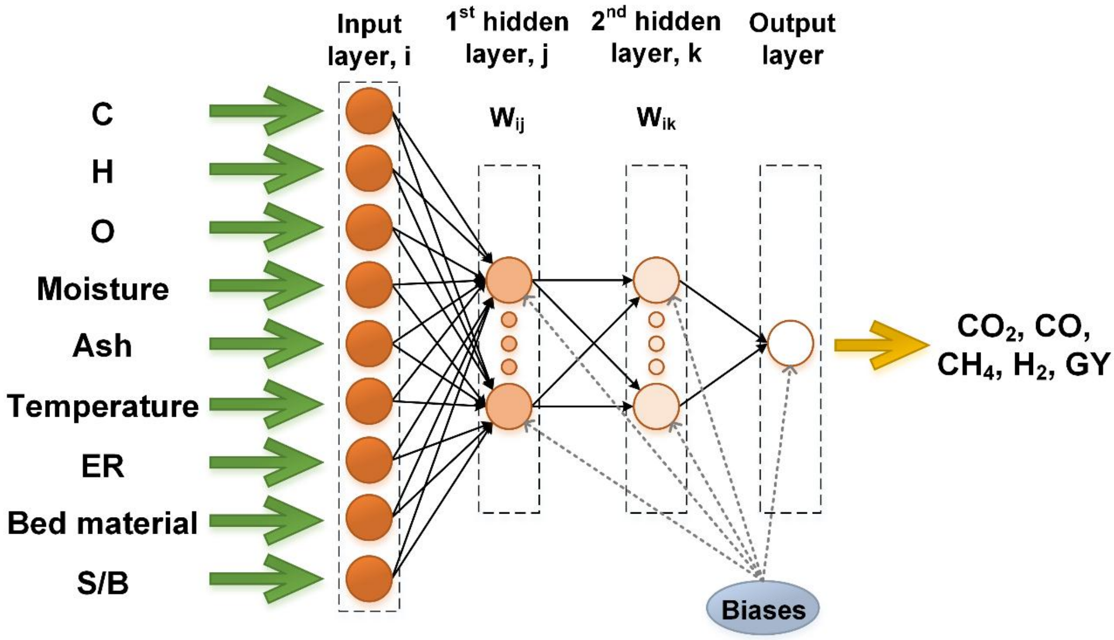

Figure 1. Proposed ANN architecture to predict the five main producer gas components in a bubbling fluidized bed gasifier.

A multi-layer feed forward and a cascade forward neural network based on back propagation (BP) learning rule with different numbers of hidden layers (one and two) were simulated using the experimental data to obtain the best prediction for the outputs during bubbling fluidized bed gasification with different bed materials. Optimal number of hidden neurons in each hidden layer has been determined for one and two hidden layers under 9–x–1 and 9–x–y–1 architectures, respectively, where x and y represents the number of neurons in the first and second hidden layer, respectively.

Table 1. Characteristics of input and output variables in the ANN based model.

Input variables	Range	Output variables	Range
C [%wt db]	27.30-85.17	GY [Nm^3/kg daf]	0.23-6.26
H [%wt db]	1.61-14.04	CH_4 [%vol N_2 free]	2.31-28.97
O [%wt db]	0-59.42	CO2 [%vol N_2 free]	2.27-58.06
Moisture [%wt ar]	0.20-27	H_2 [%vol dry]	2.60-56.88
Ash [%wt db]	0.33-44	CO [%vol N_2 free]	6.80-47.29
ER [-]	0.15-0.49		
T [ºC]	650-1050		
Bed material	1-4		
S/B [-]	0-4.04		

For bed material: 1: Silica sand; 2: Ofite; 3: Olivine; 4: Alumina
db, dry basis; ar, as received

During the BP training, the weights and biases of the different neurons are updated iteratively in order to reproduce the expected results. This algorithm uses the supervised training procedure where the network weights and biases are initialized randomly at the beginning of the training phase. The process for the error minimization is obtained using a gradient descent rule by changing the weights via an activation function for improving the performance of the network. The network minimizes the error by adjusting weights and biases until the minimum error is obtained.

The input data is repeatedly presented to the ANN and the error is computed for each repetition by comparing the output of the neural network with the desired output. Cascade forward back propagation (CFBP) operation by the use of the BP algorithm for weights updating is similar to the feed forward back propagation (FFBP) network, although the major characteristic of the network configuration is that each layer of neurons is connected to all neurons of previous layers. Levenberg-Marquardt (LM) training algorithm was applied to update the network weights. The selection of the number of hidden layers and the number of neurons in each layer is a very crucial part in the development of neural network as it improves the capacity and ability of network.

An optimum neural network architecture is proposed by varying the number of hidden layers (from 1 to 2), transfer functions and number of neurons in each hidden layer (up to 30 neurons). This selection is made considering previous works using ANNs (Pandey et al., 2016a; Puig-Arnavat et al., 2013). Different transfer functions including linear (purelin), hyperbolic tangent sigmoid (tansig) and logarithmic sigmoid (logsig) transfer functions, given in the following equations, have been utilized to reach the optimum network structure (Chayjan et al. 2014):

$$Y = A \qquad \text{(purelin)} \qquad (1)$$

$$Y = \frac{2}{(1+e^{-2A})} - 1 \qquad \text{(tansig)} \qquad (2)$$

$$Y = \frac{1}{1+e^{-A}} \qquad \text{(logsig)} \qquad (3)$$

where A_j is computed as follows:

$$A = \sum_{i=1}^{m} W_i X_i + b \qquad (4)$$

and where X_i is the input value for the i[th] input neuron, W_i is the weight between the i[th] input and the hidden layer, b is the bias for the corresponding neuron of the layer, and m is the number of input neurons. The number of transfer functions for each ANN depends on the number of hidden and output layers. Each hidden layer needs its transfer function and the same for the output layer.

In order to check the robustness, validation and prediction ability of the models, 203 data patterns obtained from different experimental conditions of experiments were randomly selected in 162 for training (80 %) and 41 for validation (20 %). These percentages are in agreement with the ones used by (Shahbaz et al., 2019). Additionally, another 10 new data patterns were used for testing (Table 3). This classification was maintained for all configurations, being the same training, validation and test data patterns in all networks. The details of ANN model parameters are presented in Table 2. Combining these parameters (network type, number of hidden layers, number of neurons and number of transfer functions), a total of 49140 ANN configurations were simulated for each output variable. The selected data for testing was presented to the trained and validated networks in order to compare the prediction performance over the same data sets.

Table 2. Details of the ANN models

No	Particulars	Specifications
1	Network type	Feed Forward Backpropagation (FFBP)
		Cascade Forward Backpropagation (CFBP)
2	Training function or Training algorithm	Levenberg-Marquardt (LM) backpropagation (TRAINLM)
3	Adaption learning function	Gradient Descent with Momentum Weight and Bias (LEARNGDM)
4	Performance function	Mean Square Error (MSE)
5	Transfer functions	Hyperbolic Tangent Sigmoid (TANSIG)
		Logarithmic sigmoid (LOGSIG)
		Linear (PURELIN)
6	Data division	Random (Dividerand)
7	Number of input layer unit	9
8	Number of output layer unit	1
9	Number of hidden layers	1 and 2
10	Number of neurons in the hidden layer	From 1 to 30
11	Number of epoch (Learning cycle)	2000 iterations

2.2. Data normalization and error evaluation

As a first step in ANN modelling to predict the outputs, all datasets (input and output) should be normalized as it increases the ability of model and the performance of the network for diagnosing relation among inputs and outputs, guaranteeing the convergence and the stability of the process (Hasanipanah et al. 2015). Data normalization has been carried out using the following equation

$$Z_{norm} = \frac{Z_r - Z_{min}}{Z_{max} - Z_{min}} \tag{5}$$

where Z_r and Z_{norm}, represent the measured and normalized values, respectively, Z_{min}, Z_{max} are the minimum and maximum values of the measured parameters, respectively.

The mean square error (MSE) and the coefficient of determination (R^2) have been used to compare the performance of the different ANN models. These parameters have been calculated by using the following equations for the experimental and ANN predictions so the best network performance is statistically obtained by the MSE and the R^2 (Chayjan et al.2014; Golpour et al. 2015):

$$MSE = \frac{1}{n}\sum_{k=1}^{n}(S_k - T_k)^2 \tag{6}$$

$$R^2 = 1 - \frac{\sum_{k=1}^{n}(S_k - T_k)^2}{\sum_{k=1}^{n}\left(S_k - \frac{\sum_{k=1}^{n} S_k}{n}\right)^2} \tag{7}$$

where S_k is the network output for k^{th} dataset, T_k is the target output for k^{th} dataset and n is the number of datasets. A low value for MSE indicates a small error between the targets and the outputs, and values or R^2 close to 1 indicates how well the model reproduces the desired outputs.

Table 3. Test data.

Test ID	C [%wt db]	H [%wt db]	O [%wt db]	Moisture [%wt]	Ash [%wt db]	ER [-]	T [ºC]	Bed material	S/B
1	50.54	7.08	41.11	8.00	0.55	0.22	800	sand	2.70
2	49.00	6.10	44.40	7.00	0.40	0.25	750	alumina	0
3	50.00	6.20	36.30	7.60	6.30	0.31	820	ofite	0
4	49.30	5.90	44.37	8.40	0.33	0.17	780	olivine	0.65
5	32.31	5.37	14.38	8.70	41.70	0.30	800	sand	1
6	27.30	4.80	18.9	7.00	44.00	0.40	850	sand	0
7	85.17	13.83	0.00	0.20	1.00	0.31	825	olivine	0
8	37.60	5.42	33.20	9.08	23.40	0.35	670	alumina	0
9	49.47	5.79	41.94	6.28	0.71	0.23	752	ofite	0.18
10	42.68	3.30	31.72	9.95	21.68	0.35	850	sand	0.8

In addition, the mean average percentage error (MAPE) was also calculated to measure the performance of the models with the test data. This value accounts for the absolute value of the average magnitude of errors in predicting each variable (Sreejith et al., 2013). This parameter, being a percentual value, is simpler to quantify and understand the error produced by the model for new data as it gives information how far the predictions are from the target values. This way, the accuracy of the prediction of new data can be better addressed.

$$MAPE = \text{—} \qquad \text{————} \tag{8}$$

3. Results and discussion

3.1. ANN using silica sand as bed material

Before analyzing the results of the different ANN using different bed materials, only datasets with silica sand as bed material (135 datasets) were used to obtain the best ANN configuration for each output. As in this case the bed material is the same for all experimental datasets, the number of inputs is reduced, having the ANN topology 8 inputs for both one and two hidden layers (8-x-1 and 8-x-y-1). Table 4 shows the results of this analysis for the different configurations in each ANN developed. The results have been selected to show the best topology and threshold functions for FFCP and CFBP, respectively. As it can be observed, configurations with one hidden layer, either FFBP or CFBP, always produced worst results than configuration with two hidden layers for all the outputs.

In the case of CO_2, the best result was obtained with a FFBP network with two hidden layers (21 and 4 neurons, respectively) and tansig-tansig-logsig as transfer functions (for the two hidden layers and the output layer). This structure generated a MSE and R^2 of $1.26 \cdot 10^{-3}$ and 0.9737, respectively. A FFBP network with two hidden layers (24 and 7 neurons, respectively) and tansig-tansig-logsig as transfer functions was the best configuration for CO prediction. The performance outputs for this architecture resulted in a MSE = $1.13 \cdot 10^{-3}$ and a R^2 = 0.9713. The most promising results for CH_4 prediction were obtained with a FFBP network with two hidden layers (3 and 22 neurons, respectively) and tansig-logsig-purelin as threshold functions. This composition produced a MSE = $7.50 \cdot 10^{-4}$ and a R^2 = 0.9553. In the case of H_2, a FFBP network with two hidden layers (23 and 19 neurons, respectively) was the best topology. The logsig transfer function was the same for all layers (hidden and output), with a MSE and R^2 values equal to $3.19 \cdot 10^{-3}$ and 0.8979, respectively. The gasification performance is measured in terms of the GY. A FFBP network with two hidden layers (19 in both first and second hidden layers) and purelin-logsig-purelin as threshold functions performed the best. In this structure, the MSE and R^2 values were $4.44 \cdot 10^{-4}$ and 0.9762, respectively.

Table 4. Best-selected topologies including different layers and neurons for FFBP and CFBP configurations using silica sand as bed material.

Element	Network	Threshold function	Topology	R^2	MSE
CO_2	FFBP	logsig-tansig	8-8-1	0.9052	$4.55 \cdot 10^{-3}$
	FFBP	**tansig-tansig-logsig**	**8-21-4-1**	**0.9737**	$\mathbf{1.26 \cdot 10^{-3}}$
	CFBP	logsig-tansig	8-5-1	0.7554	$1.17 \cdot 10^{-2}$
	CFBP	logsig-logsig-logsig	8-3-11-1	0.9627	$1.79 \cdot 10^{-3}$
CO	FFBP	logsig-purelin	8-23-1	0.8348	$6.51 \cdot 10^{-3}$
	FFBP	**tansig-tansig-logsig**	**8-24-7-1**	**0.9713**	$\mathbf{1.13 \cdot 10^{-3}}$
	CFBP	logsig-logsig	8-5-1	0.8847	$4.54 \cdot 10^{-3}$
	CFBP	purelin-tansig-purelin	8-18-27-1	0.9698	$1.19 \cdot 10^{-3}$
CH_4	FFBP	logsig-purelin	8-28-1	0.7586	$4.05 \cdot 10^{-3}$
	FFBP	**tansig-logsig-purelin**	**8-3-22-1**	**0.9553**	$\mathbf{7.50 \cdot 10^{-4}}$
	CFBP	logsig-logsig	8-16-1	0.7871	$3.57 \cdot 10^{-3}$
	CFBP	tansig-tansig-purelin	8-28-13-1	0.8264	$2.91 \cdot 10^{-3}$
H_2	FFBP	logsig-logsig	8-5-1	0.7576	$7.58 \cdot 10^{-2}$
	FFBP	**logsig-logsig-logsig**	**8-23-19-1**	**0.8979**	$\mathbf{3.19 \cdot 10^{-3}}$
	CFBP	logsig-tansig	8-11-1	0.6419	$1.12 \cdot 10^{-2}$
	CFBP	tansig-logsig-logsig	8-14-8-1	0.8869	$3.54 \cdot 10^{-3}$
GY	FFBP	logsig-purelin	8-26-1	0.6469	$6.59 \cdot 10^{-3}$
	FFBP	**purelin-logsig-purelin**	**8-19-19-1**	**0.9762**	$\mathbf{4.44 \cdot 10^{-4}}$
	CFBP	logsig-logsig	8-2-1	0.8983	$1.90 \cdot 10^{-3}$
	CFBP	logsig-tansig-purelin	8-3-15-1	0.9716	$5.30 \cdot 10^{-4}$

Once the best ANN topology for each element has been selected, the test data (Table 3) were introduced in the network to assess the accuracy of the ANN estimations. In this case, only 4 test data were used, the ones using silica sand as bed material. Figure 2a-e shows the experimental versus the predicted values, using the different ANN selected for each output. These figures also include de regression coefficient for the linear fitting. In general, all the ANN models reproduced rather good results for the testing points. In the case of H_2, the model did not estimate the testing point 6 with a good accuracy, obtaining a relative error of 90% with respect the experimental value. This leads to a very poor regression coefficient for this element. However, the rest of the points, including this one for CO_2, CO, CH_4 and GY, were near enough to the experimental ones. The MAPE for the test data is shown in Table 6, with values around 10% for CO_2, CO and CH_4, around 25% for H_2 and 2% for GY. These results can be acceptable for ANN prediction models, as also obtained in previous works (Pandey et al., 2016a; Sreejith et al., 2013).

3.2. ANN using silica sand, ofite, olivine and alumina as bed material

In this section, the effect of the bed material in the fluidized bed reactor was introduced in the model, using all datasets obtained from the literature (see supplementary information). According to the information in Table 2, 49140 ANNs have been simulated for each output variable. Table 5 shows the results in terms of MSE and R^2 for the different configurations in each ANN developed. In this case, configurations with one hidden layer, either FFBP or CFBP, also produced worst results as in the ANN using only sand as bed material.

Table 5. Best-selected topologies including different layers and neurons for FFBP and CFBP configurations using different bed materials.

Element	Network	Threshold function	Topology	R^2	MSE
CO_2	FFBP	logsig-logsig	9-2-1	0.6092	$1.31\cdot10^{-2}$
	FFBP	**tansig-tansig-logsig**	**9-16-15-1**	**0.9734**	$\mathbf{8.91\cdot10^{-4}}$
	CFBP	logsig-tansig	9-17-1	0.6745	$1.09\cdot10^{-2}$

	CFBP	tansig-tansig-logsig	9-15-24-1	0.9659	$1.14 \cdot 10^{-3}$
CO	FFBP	logsig-logsig	9-21-1	0.9544	$1.67 \cdot 10^{-3}$
	FFBP	**tansig-tansig-purelin**	**9-21-19-1**	**0.9712**	$\mathbf{1.05 \cdot 10^{-3}}$
	CFBP	logsig-logsig	9-9-1	0.8340	$6.07 \cdot 10^{-3}$
	CFBP	tansig-logsig-logsig	9-2-17-1	0.9694	$1.12 \cdot 10^{-3}$
CH_4	FFBP	logsig-tansig	9-12-1	0.7353	$6.16 \cdot 10^{-3}$
	FFBP	tansig-tansig-logsig	9-26-15-1	0.9328	$1.56 \cdot 10^{-3}$
	CFBP	logsig-logsig	9-16-1	0.9068	$2.17 \cdot 10^{-3}$
	CFBP	**tansig-tansig-logsig**	**9-7-27-1**	**0.9462**	$\mathbf{1.25 \cdot 10^{-3}}$
H_2	FFBP	logsig-logsig	9-22-1	0.4856	$1.43 \cdot 10^{-2}$
	FFBP	**tansig-tansig-logsig**	**9-5-30-1**	**0.9394**	$\mathbf{1.69 \cdot 10^{-3}}$
	CFBP	logsig-purelin	9-30-1	0.4810	$1.44 \cdot 10^{-2}$
	CFBP	purelin-logsig-logsig	9-24-21-1	0.9231	$2.14 \cdot 10^{-3}$
GY	FFBP	logsig-purelin	9-3-1	0.7676	$5.28 \cdot 10^{-3}$
	FFBP	**tansig-tansig-logsig**	**9-18-19-1**	**0.9872**	$\mathbf{2.90 \cdot 10^{-4}}$
	CFBP	tansig-purelin	9-2-1	0.7699	$5.23 \cdot 10^{-3}$
	CFBP	logsig-logsig-logsig	9-8-10-1	0.9843	$5.56 \cdot 10^{-4}$

The best result for CO_2 was obtained with a FFBP network with two hidden layers with 16 and 15 neurons, respectively. The threshold function for this network was tansig-tansig-logsig. This structure generated a MSE = $8.91 \cdot 10^{-4}$ and R^2 = 0.9734. According to the results (not presented here), another FF network configuration produced rather similar results with a R^2 higher than 0.97, with different transfer functions and neurons configuration. In the case of CO, a FFBP network with two hidden layers (21 and 19 neurons) and tansig-tansig-purelin as threshold functions was the best configuration. The performance outputs for this architecture resulted in a MSE = $1.05 \cdot 10^{-3}$ and R^2 = 0.9712. In this case, the FFBP configuration with one hidden layer also produced rather good results (R^2 higher than 0.95). The most promising results for CH_4 were obtained with a CFBP network, two hidden layers with 7 and 27 neurons, respectively, and tansig-tansig-logsig threshold functions. This composition produced a MSE = $1.25 \cdot 10^{-3}$ and R^2 = 0.9462. The best configuration for H_2 was a FFBP network with two hidden layers (5 and 30 neurons, respectively) and tansig-tansig-logsig threshold functions, with a MSE and R^2 values equal to $1.69 \cdot 10^{-3}$ and 0.9394, respectively. Up to 12 network FF topologies also resulted in R^2 values higher than 0.93. In the case of GY, the best configuration was a FFBP network with two hidden layers (18 and 19 neurons, respectively) and tansig-tansig-logsig as threshold functions. In this structure, the MSE and R^2 values were $2.90 \cdot 10^{-4}$ and 0.9872, respectively.

Figure 2f-j shows the results when the test data (Table 3) was introduced in the different models. In this case, the regression coefficients were a bit worse than in the previous case using silica sand as bed material, influenced by the higher number of test data and the higher complexity of the ANNs as they have to differentiate between different bed materials. Then, the test data produced rather good correlation between experimental and predicted data, been most of the test points below a relative error of 10%. It can be observed that for each output the test data points with higher error are not always the same. Although test number 4 (olivine as bed material) is always quite far from the experimental target. Attending to the MAPE, this parameter resulted in higher values than in the previous scenario with silica sand as bed material. Due to the higher complexity of the models and the heterogeneity of the data, these results could be satisfactory.

Table 6. MAPE for the test data in the different ANN models.

	CO_2	**CO**	**CH_4**	**H_2**	**GY**
Silica sand as bed material					
	8.78	12.54	12.21	24.89	2.25
Silica sand, ofite, olivine and alumina as bed materials					
	28.21	27.30	38.91	15.64	8.18

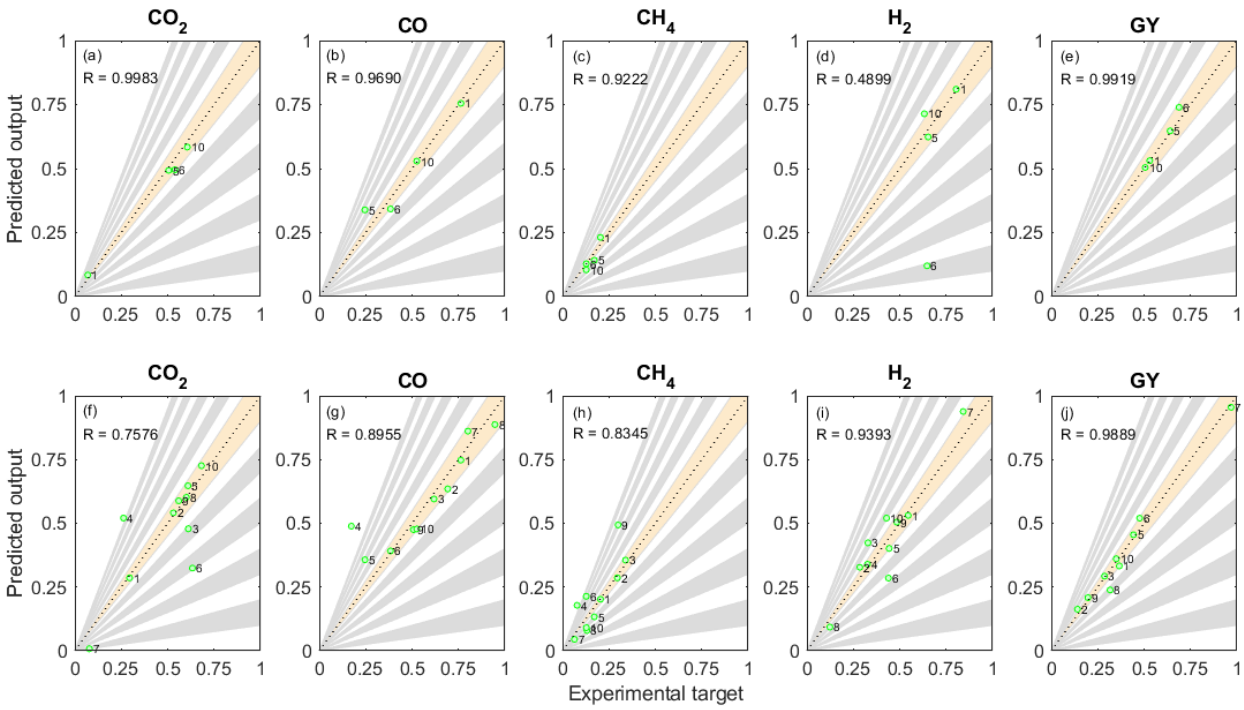

Figure 2. Testing results for the selected ANNs: (a)-(e) using silica sand as bed material; (f)-(j) using all bed materials. Each shadowed region corresponds with a relative error of 10%.

The R values shows a good fitting during training and validation, while for testing process that indicator is a bit worse due to the big error introduced with test data set 4. It is clearly apparent that the accuracy of the network during the training process is better than testing or validation. During the training process, the network modifies the values of its input and output weights to get the best fitness whereas in the testing or validation process the output shows the actual predictive performance of the trained model on new data without adjusting the weights. Therefore, the observed R^2 and MSE values show a good indication of well-trained ANN model. The performance of the model is an indication of the appropriate selection of the input variables.

The obtained networks are highly accurate and consume a short time to obtain the results. These findings are in agreement with the reported results in the literature (Souza et al., 2012). It can be stated that ANN are powerful tools for gasification modeling in different conditions.

4. Conclusions

The FFBP models with two hidden layers show an improved performance over the CFBP models and those with only one hidden layer to predict product gas composition in terms of CO_2, CO, CH_4, H_2 and GY, producing a higher coefficient of determination (R^2). The results show that the degree of agreement between experimental and predicted values justifies the accuracy of the proposed ANN models. Therefore, for a given bubbling fluidized bed gasifier, the developed models are capable of simulate the producer gas composition for selected biomasses at specified operating conditions, including the effect of the bed material in the reactor.

Supplementary information

E-supplementary data associated with this work can be found in online version of the paper.

Abbreviations

ANN	artificial neural network
BP	back propagation
CFBP	cascade forward back propagation
CFD	computational fluid dynamics
ER	equivalence ratio
FFBP	feed forward back propagation
GY	gas yield
LM	Levenberg-Marquardt

MAPE mean average percentage error

MC moisture content

MSE mean square error

R^2 determination coefficient

References

Ahmed, T.Y., Ahmad, M.M., Yusup, S., Inayat, A., Khan, Z., 2012. Mathematical and computational approaches for design of biomass gasification for hydrogen production: A review. Renew. Sustain. Energy Rev. https://doi.org/10.1016/j.rser.2012.01.035

Arena, U., Di Gregorio, F., 2014. Gasification of a solid recovered fuel in a pilot scale fluidized bed reactor. Fuel 117, 528–536. https://doi.org/10.1016/j.fuel.2013.09.044

Arena, U., Zaccariello, L., Mastellone, M.L., 2010. Fluidized bed gasification of waste-derived fuels. Waste Manag. 30, 1212–1219. https://doi.org/10.1016/j.wasman.2010.01.038

Ayodele, B. V, Cheng, C.K., 2015. Modelling and optimization of syngas production from methane dry reforming over ceria-supported cobalt catalyst using artificial neural networks and Box-Behnken design. J. Ind. Eng. Chem. 32, 246–258. https://doi.org/10.1016/j.jiec.2015.08.021

Baratieri, M., Pieratti, E., Nordgreen, T., Grigiante, M., 2010. Biomass gasification with dolomite as catalyst in a small fluidized bed experimental and modelling analysis. Waste and Biomass Valorization 1, 283–291. https://doi.org/10.1007/s12649-010-9034-6

Baruah, D., Baruah, D.C., 2014. Modeling of biomass gasification: A review. Renew. Sustain. Energy Rev. https://doi.org/10.1016/j.rser.2014.07.129

Baruah, D., Baruah, D.C., Hazarika, M.K., 2017. Artificial neural network based modeling of biomass gasification in fixed bed downdraft gasifiers. Biomass and Bioenergy 98, 264–271. https://doi.org/10.1016/j.biombioe.2017.01.029

Campoy Naranjo, M., 2009. Biomass and waste gasification in fluidised bed: pilot plant studies.

University of Seville.

Chavan, P.D., Sharma, T., Mall, B.K., Rajurkar, B.D., Tambe, S.S., Sharma, B.K., Kulkarni, B.D., 2012. Development of data-driven models for fluidized-bed coal gasification process. Fuel 93, 44–51. https://doi.org/10.1016/j.fuel.2011.11.039

Chayjan, R.A., Kaveh, M., Khayati, S., 2014. Modeling some drying characteristics of sour cherry (Prunus cerasus L.) under infrared radiation using mathematical models and artificial neural networks. Agric. Eng. Int. CIGR J. 16, 265–279.

Christodoulou, C., Grimekis, D., Panopoulos, K.D., Pachatouridou, E.P., Iliopoulou, E.F., Kakaras, E., 2014. Comparing calcined and un-treated olivine as bed materials for tar reduction in fluidized bed gasification. Fuel Process. Technol. 124, 275–285. https://doi.org/10.1016/j.fuproc.2014.03.012

De Andrés, J.M., Narros, A., Rodríguez, M.E., 2011a. Behaviour of dolomite, olivine and alumina as primary catalysts in air-steam gasification of sewage sludge. Fuel 90, 521–527. https://doi.org/10.1016/j.fuel.2010.09.043

De Andrés, J.M., Narros, A., Rodríguez, M.E., 2011b. Air-steam gasification of sewage sludge in a bubbling bed reactor: Effect of alumina as a primary catalyst. Fuel Process. Technol. 92, 433–440. https://doi.org/10.1016/j.fuproc.2010.10.006

Golpour, I., Amiri Chayjan, R., Amiri Parian, J., Khazaei, J., 2015. Prediction of paddy moisture content during thin layer drying using machine vision and artificial neural networks. J. Agric. Sci. Technol. 17, 287–298.

Gómez-Barea, A., Arjona, R., Ollero, P., 2005. Pilot-plant gasification of olive stone: A technical assessment. Energy and Fuels 19, 598–605. https://doi.org/10.1021/ef0498418

Guo, B., Li, D., Cheng, C., Lü, Z.A., Shen, Y., 2001. Simulation of biomass gasification with a hybrid neural network model. Bioresour. Technol. 76, 77–83. https://doi.org/10.1016/S0960-8524(00)00106-1

Hasanipanah, M., Jahed Armaghani, D., Khamesi, H., Bakhshandeh Amnieh, H., Ghoraba, S., 2016. Several non-linear models in estimating air-overpressure resulting from mine blasting. Eng. Comput. 32, 441–455. https://doi.org/10.1007/s00366-015-0425-y

Huynh, C. Van, Kong, S.C., 2013. Performance characteristics of a pilot-scale biomass gasifier using oxygen-enriched air and steam, in: Fuel. https://doi.org/10.1016/j.fuel.2012.09.033

Kaewluan, S., Pipatmanomai, S., 2011a. Potential of synthesis gas production from rubber wood chip gasification in a bubbling fluidised bed gasifier. Energy Convers. Manag. 52, 75–84. https://doi.org/10.1016/j.enconman.2010.06.044

Kaewluan, S., Pipatmanomai, S., 2011b. Gasification of high moisture rubber woodchip with rubber waste in a bubbling fluidized bed. Fuel Process. Technol. https://doi.org/10.1016/j.fuproc.2010.11.026

Karaci, A., Caglar, A., Aydinli, B., Pekol, S., 2016. The pyrolysis process verification of hydrogen rich gas (H-rG) production by artificial neural network (ANN). Int. J. Hydrogen Energy 41, 4570–4578. https://doi.org/10.1016/j.ijhydene.2016.01.094

Karmakar, M.K., Datta, A.B., 2011. Generation of hydrogen rich gas through fluidized bed gasification of biomass. Bioresour. Technol. 102, 1907–1913. https://doi.org/10.1016/j.biortech.2010.08.015

Lahijani, P., Zainal, Z.A., 2011. Gasification of palm empty fruit bunch in a bubbling fluidized bed: A performance and agglomeration study. Bioresour. Technol. 102, 2068–2076. https://doi.org/10.1016/j.biortech.2010.09.101

Lan, W., Chen, G., Zhu, X., Wang, Xin, Wang, Xuetao, Xu, B., 2019. Research on the characteristics of biomass gasification in a fluidized bed. J. Energy Inst. 92, 613–620. https://doi.org/10.1016/j.joei.2018.03.011

Loha, C., Chattopadhyay, H., Chatterjee, P.K., 2013. Energy generation from fluidized bed gasification of rice husk. J. Renew. Sustain. Energy 5, 043111. https://doi.org/10.1063/1.4816496

Lv, P.M., Xiong, Z.H., Chang, J., Wu, C.Z., Chen, Y., Zhu, J.X., 2004. An experimental study on biomass air-steam gasification in a fluidized bed. Bioresour. Technol. 95, 95–101. https://doi.org/10.1016/j.biortech.2004.02.003

Mahishi, M.R., Goswami, D.Y., 2007. Thermodynamic optimization of biomass gasifier for hydrogen production. Int. J. Hydrogen Energy 32, 3831–3840.

https://doi.org/10.1016/j.ijhydene.2007.05.018

Mansaray, K.G., Ghaly, A.E., Al-Taweel, A.M., Hamdullahpur, F., Ugursal, V.I., 1999. Air gasification of rice husk in a dual distributor type fluidized bed gasifier. Biomass and Bioenergy 17, 315–332. https://doi.org/10.1016/S0961-9534(99)00046-X

Miccio, F., Piriou, B., Ruoppolo, G., Chirone, R., 2009. Biomass gasification in a catalytic fluidized reactor with beds of different materials. Chem. Eng. J. 154, 369–374. https://doi.org/10.1016/j.cej.2009.04.002

Mikulandrić, R., Lončar, D., Böhning, D., Böhme, R., Beckmann, M., 2014. Artificial neural network modelling approach for a biomass gasification process in fixed bed gasifiers. Energy Convers. Manag. 87, 1210–1223. https://doi.org/10.1016/j.enconman.2014.03.036

Narváez, I., Orío, A., Aznar, M.P., Corella, J., 1996. Biomass gasification with air in an atmospheric bubbling fluidized bed. Effect of six operational variables on the quality of the produced raw gas. Ind. Eng. Chem. Res. 35, 2110–2120. https://doi.org/10.1021/ie9507540

Pandey, D.S., Das, S., Pan, I., Leahy, J.J., Kwapinski, W., 2016a. Artificial neural network based modelling approach for municipal solid waste gasification in a fluidized bed reactor. Waste Manag. 58, 202–213. https://doi.org/10.1016/j.wasman.2016.08.023

Pandey, D.S., Kwapinska, M., Gómez-Barea, A., Horvat, A., Fryda, L.E., Rabou, L.P.L.M., Leahy, J.J., Kwapinski, W., 2016b. Poultry Litter Gasification in a Fluidized Bed Reactor: Effects of Gasifying Agent and Limestone Addition. Energy and Fuels 30, 3085–3096. https://doi.org/10.1021/acs.energyfuels.6b00058

Puig-Arnavat, M., Bruno, J.C., Coronas, A., 2010. Review and analysis of biomass gasification models. Renew. Sustain. Energy Rev. 14, 2841–2851. https://doi.org/10.1016/j.rser.2010.07.030

Puig-Arnavat, M., Hernández, J.A., Bruno, J.C., Coronas, A., 2013. Artificial neural network models for biomass gasification in fluidized bed gasifiers. Biomass and Bioenergy 49, 279–289. https://doi.org/10.1016/j.biombioe.2012.12.012

Roche, E., De Andrés, J.M., Narros, A., Rodríguez, M.E., 2014. Air and air-steam gasification of sewage sludge. The influence of dolomite and throughput in tar production and composition. Fuel 115, 54–61. https://doi.org/10.1016/j.fuel.2013.07.003

Serrano, D., Kwapinska, M., Horvat, A., Sánchez-Delgado, S., Leahy, J.J., 2016. Cynara cardunculus L. gasification in a bubbling fluidized bed: The effect of magnesite and olivine on product gas, tar and gasification performance. Fuel 173, 247–259. https://doi.org/10.1016/j.fuel.2016.01.051

Serrano, D., Sánchez-Delgado, S., Horvat, A., 2017. Effect of sepiolite bed material on gas composition and tar mitigation during C. cardunculus L. gasification. Chem. Eng. J. 317, 1037–1046. https://doi.org/10.1016/j.cej.2017.02.106

Shahbaz, M., Taqvi, S.A., Minh Loy, A.C., Inayat, A., Uddin, F., Bokhari, A., Naqvi, S.R., 2019. Artificial neural network approach for the steam gasification of palm oil waste using bottom ash and CaO. Renew. Energy. https://doi.org/10.1016/j.renene.2018.07.142

Souza, M.B. de, Couceiro, L., Barreto, A.G., B. Quitete, C.P., 2012. Neural Network Based Modeling and Operational Optimization of Biomass Gasification Processes, in: Yun, Y. (Ed.), Gasification for Practical Applications. https://doi.org/10.5772/48516

Sreejith, C.C., Muraleedharan, C., Arun, P., 2013. Performance prediction of fluidised bed gasification of biomass using experimental data-based simulation models. Biomass Convers. Biorefinery 3, 283–304. https://doi.org/10.1007/s13399-013-0083-5

Sunphorka, S., Chalermsinsuwan, B., Piumsomboon, P., 2017. Artificial neural network model for the prediction of kinetic parameters of biomass pyrolysis from its constituents. Fuel 193, 142–158. https://doi.org/10.1016/j.fuel.2016.12.046

Xiao, G., Ni, M. jiang, Chi, Y., Jin, B. sheng, Xiao, R., Zhong, Z. ping, Huang, Y. ji, 2009. Gasification characteristics of MSW and an ANN prediction model. Waste Manag. 29, 240–244. https://doi.org/10.1016/j.wasman.2008.02.022